



**HAL**  
open science

# Robust Electroencephalogram Phase Estimation with Applications in Brain-computer Interface Systems

Esmail Seraj, Reza Sameni

► **To cite this version:**

Esmail Seraj, Reza Sameni. Robust Electroencephalogram Phase Estimation with Applications in Brain-computer Interface Systems. 2016. hal-01378726v1

**HAL Id: hal-01378726**

**<https://hal.science/hal-01378726v1>**

Preprint submitted on 10 Oct 2016 (v1), last revised 19 Oct 2017 (v2)

**HAL** is a multi-disciplinary open access archive for the deposit and dissemination of scientific research documents, whether they are published or not. The documents may come from teaching and research institutions in France or abroad, or from public or private research centers.

L'archive ouverte pluridisciplinaire **HAL**, est destinée au dépôt et à la diffusion de documents scientifiques de niveau recherche, publiés ou non, émanant des établissements d'enseignement et de recherche français ou étrangers, des laboratoires publics ou privés.

# Robust Electroencephalogram Phase Estimation with Applications in Brain-computer Interface Systems

Esmail Seraj and Reza Sameni\*

Signal Processing Center, Department of Computer Science and Information Technology, School of Electrical and Computer Engineering, Shiraz University, Shiraz, Iran.

Tel: +98 71 3613 3169, Fax: +98 71 3647 4605, E-mail: e.seraj@cse.shirazu.ac.ir, rsameni@shirazu.ac.ir

---

## Abstract

In this study, a robust method is developed for frequency-specific electroencephalogram (EEG) phase extraction using the analytic representation of the EEG. Using recent theoretical findings in this area, it is shown that some of the phase variations— previously associated to the brain response— are systematic side-effects of the methods used for EEG phase calculation, especially during low analytical amplitude segments of the EEG.

With this insight, the proposed method generates randomized ensembles of the EEG phase using minor perturbations in pole-zero loci of narrow-band zero-phase IIR filters, followed by phase estimation using the signal's analytical form and ensemble averaging to obtain a robust EEG phase. This Monte Carlo method is shown to be very robust to noise and minor changes of the filter parameters and reduces the effect of fake EEG phase jumps (without a cerebral source).

As proof of concept, the proposed method is used for extracting EEG phase features in brain computer interface (BCI) classification. The results show significant improvement in classification rates using rather simple phase-related features over a standard BCI dataset.

The proposed method for EEG phase calculation is very generic and may be applied for all EEG phase-related studies.

**Keywords:** Electroencephalogram Phase; Narrow-Band Electroencephalography; Phase Extraction; Analytic Signals; Brain-computer Interface.

---

## 1. Introduction

The phase analysis of electroencephalogram (EEG) signals has found great interest in the past decades. It has been shown to be a considerable (and in cases more informative) complement for the EEG spectral amplitude. In [1], various methods were presented for extracting the instantaneous EEG phase and amplitude of real EEG signals. The relationship between the different methods were studied using the theory of *analytic signals*. In [2], the relation between phase synchronization in EEG signals and brain activity in patients with temporal lobe epilepsy was investigated. The authors reported a strong correlation between shifts in phase synchrony and pathological activity. In [3], the concept of Frequency Flows Analysis (*FFA*) was introduced, as a new approach for studying the dynamics of phase synchrony in brain signals. The application of EEG phase and phase synchrony in brain recordings for brain-computer interface (BCI) systems was studied in [4]. It was reported that additional information could be available by utilizing phase-related quantities for measuring brain synchrony. Other studies such as [5] and [6] studied two other important phase related quantities, namely *phase shift* and *phase resetting* and their relations to components of event related potentials. In [7], an *empirical mode decomposition* (EMD) based method was proposed along with phase synchronization and evaluated in BCI systems. The phase-locking value (PLV) has been previously

utilized to associate the EEG phase information in BCI systems [8]. Various methods such as *wavelet transforms* and *analytic signal representation* of signals have been used for EEG phase extraction and PLV measurement [9, 10].

In a recent study [11], the authors presented a statistical framework for EEG phase analysis. Using an additive data model between the so called background (spontaneous) and foreground EEG, probability density functions and other statistical properties of the instantaneous EEG envelope, phase and frequency were derived. It was analytically and numerically shown that in low analytical signal envelopes, the EEG phase is highly noisy and susceptible to the background EEG activity. It was shown that although EEG phase variations convey important information regarding the EEG, some instantaneous phase jumps are systematic side effects of the processing stages used for EEG phase extraction in low analytical envelopes and are not related to the brain. A Monte Carlo approach was proposed in [11] to detect and smooth the time instants in which the estimated EEG phase is unreliable.

In this contribution, using our recent findings reported in [11], a new EEG phase extraction procedure is presented, for extracting reliable phase sequences from the EEG for BCI applications. It is shown that the discrimination between true and fake EEG phase variations can significantly improve classification rates in BCI applications, even using rather basic features

and conventional classifiers.

In the following section, some preliminary backgrounds and the limitations of classical stages of EEG phase extraction are reviewed. In Section 3, some modifications are proposed for the conventional procedure of instantaneous EEG phase extraction. For proof of concept, the proposed method is used for feature extraction in a BCI application, showing significant improvement in the classification rates.

## 2. Background

### 2.1. Conventional Phase Estimation Procedure

The conventional procedure for extracting the instantaneous phase sequence of a signal contains two main stages: 1) narrow-band filtering and 2) estimating the phase of the narrow-band signal [12, 13].

For a unique and canonical definition, the instantaneous phase is extracted from very narrow frequency band signals [14]. Moreover, the input signal's phase contents should not be affected by the filtering procedure. For the first stage, almost all previous studies on EEG phase extraction have used finite impulse response (FIR) filters to make the signal narrow-band in its frequency spectrum [2, 15, 16, 8, 9, 17]. However, in order to have a reliable phase sequence, there are important considerations regarding this procedure, including: the filter's bandwidth, its phase response and the convolution process. The underlying theories and practical issues in this regard are reviewed in the next section.

The second stage requires choosing a phase estimation method to extract the phase sequence from the narrow-band signal. Apparently, accurate methods that do not violate theoretical conditions essential for having a reliable instantaneous phase should be used at this stage. The most common method for phase estimation is through using the *analytic signal* representation of the narrow-band signal [14]. As shown in [11], the calculation of the instantaneous phase from the analytical representations becomes challenging and highly susceptible to noise in low analytical signal amplitudes; resulting in fake jumps and spikes in the extracted phase signal. In the following sections, this issue is further studied and partially solved by applying perturbations in the phase extraction procedure as proposed in [11].

### 2.2. Unambiguous Phase Estimation Conditions

The most common definition of the instantaneous phase is based on the analytic representation of a signal [14]. Accordingly, for the signal  $x(t)$ , its analytical form is defined as follows [13]:

$$z_x(t) = x(t) + jH\{x(t)\} \quad (1)$$

where  $H\{x(t)\}$  is the Hilbert transform of  $x(t)$ . Using the analytical form of a narrow band signal, the instantaneous envelope and phase pair are uniquely defined as follows:

$$a_x(t) = |z_x(t)| = \sqrt{x(t)^2 + H\{x(t)\}^2} \quad (2)$$

$$\phi_x(t) = \arctan\left(\frac{H\{x(t)\}}{x(t)}\right) \quad (3)$$

Unless the signal has a narrow-band spectral support, the pair  $(a_x(t), \phi_x(t))$  do not convey significant information regarding the instantaneous phase [12]. This mainly raises from the fact that for narrow-band signals, the relative variations of the amplitude  $a_x(t)$  are rather slow as compared with the variations of the phase  $\phi_x(t)$  [13], i.e.,

$$\left|\frac{d\phi(t)}{dt}\right| \gg \left|\frac{1}{a(t)} \frac{da(t)}{dt}\right| \quad (4)$$

This condition is well-satisfied if the signal is narrow-band in its spectral support.

For cerebral signals, it is known that the EEG has a wide frequency range (0 Hz-150 Hz in the extreme case) which makes narrow-bandpass filtering an essential prerequisite for extracting a meaningful instantaneous phase sequence.

### 2.3. Linear-phase Filtering

Previous studies on EEG phase extraction have commonly employed linear-phase filters to make the signal narrow-band in its frequency spectrum [2, 15, 16, 8, 9, 17]. The advantage of linear phase filters is their constant group delay, which avoids phase distortions of the filtered signal. Nevertheless, in most FIR filter design techniques, the order of the filter proportionally increases with the inverse of their transition bandwidth, which means that narrow-band FIR filters have very long impulse responses and input-output delays. Moreover, highly narrow band filters are difficult to design and susceptible to design parameters.

To avoid these issues, previous studies have kept a trade-off between the order of the FIR filter and its band-width (*BW*). Mainly, the *BW* was chosen relatively large (e.g., between 4 to 12 Hz), to have a low-order and practically realizable filter [2, 18, 17]. However, as discussed before, using a bandwidth in this range, the envelope-phase pair  $\{a(t), \phi(t)\}$  obtained from the Hilbert transform fails to correctly/uniquely define the instantaneous envelope and phase and the extracted phase will not be reliable. Therefore, very narrow band filters with reasonably low orders are required in practice to be less sensitive to noise and variations in its parameters and is indispensable.

### 2.4. Low-amplitude Analytical Signal

The instantaneous phase sequence derived from the analytic representation of signal is prone to contain fake (without cerebral source) jumps in Low Amplitude Analytical Signal (LAAS) time instants [13, 14, 17]. As depicted in Fig. 1, the instantaneous frequency tends to have big jumps at LAAS epochs.

The problem was rigorously studied in [11]. The main reason underlying this phenomenon could be linked to the  $\arctan(\cdot)$  operator for phase calculation. According to (3), LAAS causes the denominator to be very low. Consequently, any minor change in the real or imaginary parts of the analytic form (due to noise or background EEG fluctuations), leads to a significant change in the estimated phase. This is illustrated in Fig. 2. It is seen that phase values corresponding to lower amplitudes tend to have bigger alterations due to a small additive noise. It was shown

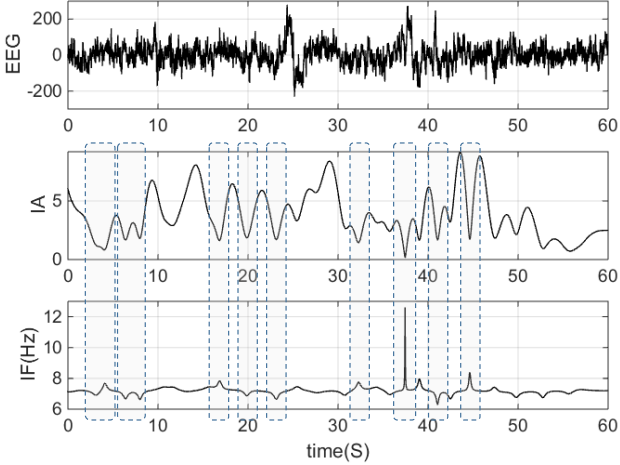


Figure 1: A raw 60 s EEG signal used for phase extraction (top panel), the analytical signal envelope derived from analytic form of signal (middle panel), and the corresponding instantaneous frequency centered at 7 Hz obtained from the phase sequence extracted through the analytic signal (bottom panel).

in [11] that during LASS epochs the instantaneous phase tends to a uniform distribution over  $[-\pi, \pi]$  and the instantaneous frequency becomes uniform over the entire Nyquist band.

The findings of [11] is in accordance with [17], which reported that LAAS occurs more frequently in low power time-frequency regions (especially high frequency bands of the EEG); since the EEG power decays more rapidly with increasing frequency. To illustrate this point, in Fig. 3 the instantaneous phase differences of frequency components in the range of DC to 50 Hz have been extracted alongside with their corresponding instantaneous envelopes. Accordingly, the first 5 s of the results are due to the FIR filter’s transient response; resulting in very low-magnitude instantaneous amplitude signals during this period. As it can be seen, the corresponding regions of the phase difference plot contains many phase jumps and spikes. For the rest of the signal, in lower frequencies, where the analytic form has higher amplitudes, the phase sequences are less contaminated with jumps and spikes. However, as the frequency increases and the power in EEG signal decays (the analytical signal envelope decreases), the rate of phase jumps increases once more.

Based on these findings, in the next section a robust method is proposed for the estimation of the instantaneous phase using perturbation of filter parameters and Monte Carlo simulation.

### 3. Method

The proposed method for robust EEG phase extraction consists of successive steps, which are separately detailed in the following sections. The overall scheme is summarized in Algorithm 1.

#### 3.1. Step (1): Narrow-band zero-phase smoothing

To overcome the issues associated with FIR filters, we propose using forward-backward zero-phase IIR filters. Although the filter is performed offline in a non-causal manner, the major

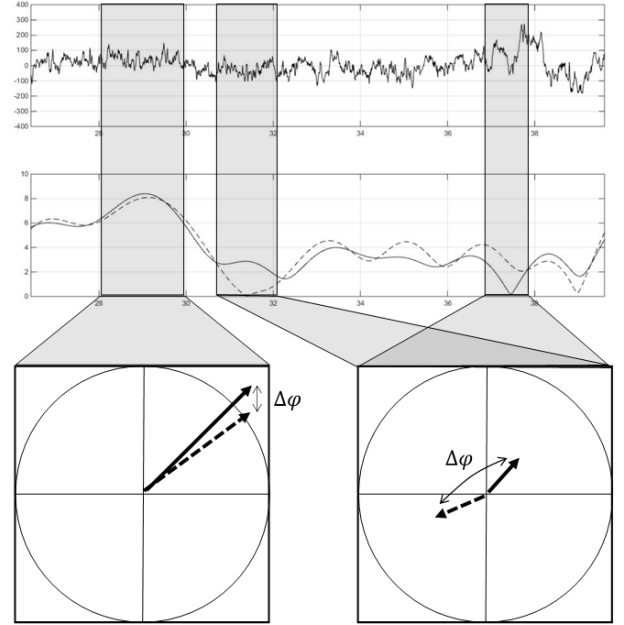


Figure 2: A 14 s segment of a raw EEG signal used for extracting instantaneous phase sequence (top panel), the analytical signal envelope derived from the clean signal (middle panel, solid black line), and contaminated with additive white noise (middle panel dashed line), and the estimated phase during two segments with low and high analytic signal envelope (bottom panel). The solid and dashed arrows show the results for the analytical signal envelope obtained from clean and noisy EEG signals, respectively.

advantage is that the order of a narrow band IIR filters is much lower than its FIR counterpart and by applying it in a forward-backward manner, the nonlinear phase response of the filter is compensated and zero-phase distortion— which is necessary for EEG phase analysis— is guaranteed.

Various types of IIR filters such as *Chebyshev types 1, 2*, *Butterworth* and *Elliptic* were studied to determine the best filter for this application and the Elliptic filter was chosen due to its steeper roll-off characteristics (as compared with Butterworth or Chebyshev filters) and its equi-ripple feature in both the passband and stopband. In general, by allowing ripples in both passband and stopbands, Elliptic filters meet given performance specifications with the lowest order as compared with their counterparts [19]. In order to preserve the filter’s frequency response over all frequency bands, instead of designing various bandpass filters in each band, a fixed narrow band low-pass filter prototype was designed and shifted in the frequency domain in a mixer-like manner. The prototype Elliptic IIR low-pass filter used in this study has the characteristics of 0.3 Hz pass-band, 0.5 Hz stop-band, 0.1 dB maximum pass-band ripple and 70 dB minimum stop-band attenuation, at a sampling frequency of 160 Hz. The order of this prototype filter was 6, which is far more effective than any FIR filter with the same specifications. This filter was performed in a forward backward manner, which doubles its pass-band ripple and stop band attenuation in dB.

The procedure of zero-phase forward-backward smoothing (FBS) is as shown in Fig. 4. Accordingly, FBS uses the time-

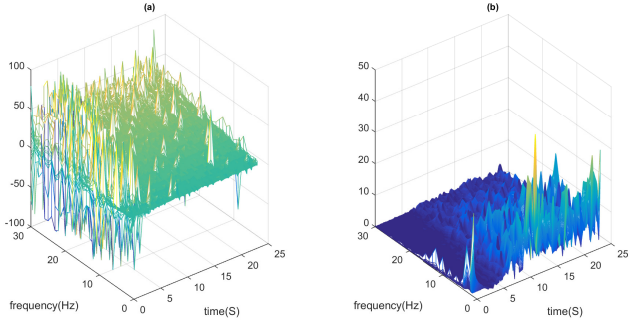


Figure 3: Phase difference of the frequency components from DC to 50 Hz (left panel), the corresponding instantaneous analytical signal envelope (right panel).

---

### Algorithm 1 Robust Instantaneous EEG Phase Extraction

---

**Require:** Discrete-time EEG signal  $x(t)$

**Require:** Bandpass filter prototype  $h_{BP}(t)$  with design parameters  $\{BW, TB, PR, SR\}$  and pole-zero sets  $P$  and  $Z$ , respectively.

**Require:** Number of perturbation iterations ( $N$ )

- 1: **for all**  $i = 1 \cdots N$  **do**
  - 2: Perturb the poles and zeros with minor random deviations  $\delta_i^p$  and  $\delta_i^z$ , while keeping the pole-zeros conjugate symmetric and preserving the poles inside the unit circle:  $P_i \leftarrow P \pm \delta_i^p, Z_i \leftarrow Z \pm \delta_i^z$
  - 3: Construct the new bandpass filter with the perturbed pole zero pairs  $P_i$  and  $Z_i$
  - 4: Zero-phase forward-backward filter<sup>1</sup> the input signal  $x_i(t) = ZPF_i\{x(t)\}$
  - 5: Form the analytic representation of filtered signal  $z_i(t) = Re\{x_i(t)\} + jIm\{x_i(t)\}$
  - 6: Calculate the instantaneous phase using the analytic form  $\phi_i(t) = \arctan\left(\frac{Im\{z_i(t)\}}{Re\{z_i(t)\}}\right)$
  - 7: **end for**
  - 8: Unwrap the estimated phase sequences  $\Phi_i(t) \leftarrow \text{unwrap}\{\phi_i(t)\}$
  - 9: Ensemble average over all  $i$ :  $\Phi(t) \leftarrow \frac{1}{N} \sum_{i=1}^N \Phi_i(t)$
- 

reversal property of the Fourier transform to perform zero-phase smoothing by processing the input signal in both the forward and reverse directions [20]. Considering  $H(e^{j\omega})$  as the frequency response of the forward path digital filter, the effective response of FBS is

$$H_{eff}(e^{j\omega}) = |H(e^{j\omega})|^2 \quad (5)$$

which is the real-valued. Therefore, regardless of the nonlinear phase-response of the IIR filter, FBS has a zero-phase (and zero-group delay) frequency response, which preserves the input signal's phase.

### 3.2. Step (2): Phase Calculation

The next step is to compute the phase sequence. For this, we use the analytic representation of the filtered signal. In order to reduce the processing complexity and avoid the direct

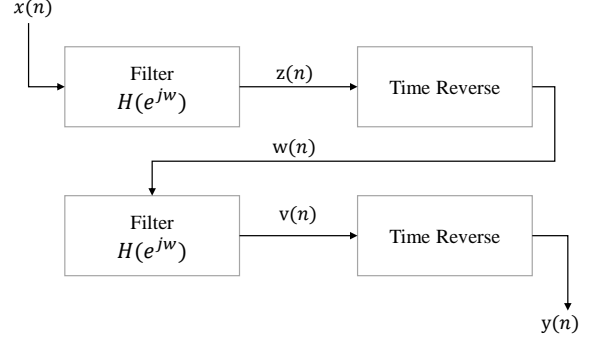


Figure 4: Block-diagram of the forward-backward filtering process.

calculation of the Hilbert transform, this stage can be merged with the bandpass filtering as follows: as noted before, the proposed bandpass filtering scheme uses a lowpass filter prototype. To filter the signal  $x(t)$  around the center frequency  $\omega_0$ ,  $x(t)$  is shifted in the frequency by multiplying the pure phase signal  $\exp(-j\omega_0 t)$ , to obtain a complex valued signal  $x_f(t)$ . Next, the real and imaginary parts of  $x_f(t)$  are given to the lowpass prototype to obtain the narrow-band analytical signal  $y_f(t)$ . Finally,  $y_f(t)$  is shifted back to the center frequency  $\omega_0$ , by multiplying the phase signal  $\exp(j\omega_0 t)$ . This procedure provides  $x_a(t)$ , which is the narrow band analytical form of the original signal  $x(t)$  around the center frequency  $\omega_0$ .

After computing the analytic form of the filtered EEG signal, here presented as  $x(t)$ , its phase sequence can be measured as follow:

$$\phi(t) = \arctan\left(\frac{Im(x_a(t))}{Re(x_a(t))}\right) \quad (6)$$

For discrete-time signals, the instantaneous frequency can be approximated by the first order difference of the instantaneous phase:

$$f(t) = f_s \frac{\phi(t) - \phi(t - \Delta)}{2\pi} \quad (7)$$

where  $\Delta$  is the sampling time and  $f_s = 1/\Delta$  is the sampling frequency.

### 3.3. Step (3): Zero-pole Perturbation of the Filter

The previous two stages (narrow band filtering and phase calculation) are applied several times with very minor changes in the filter design parameters, as proposed in [11]. Here, the idea is to generate random ensembles of the signal's analytical form and EEG phase, using infinitesimal perturbations parameter variations. Apparently, clinically relevant EEG phase information should not be susceptible to minor filter design variations at the order of, e.g., 0.01 Hz. However, at during LAAS epochs, even minor deviations in the filter parameters can significantly change the phase estimates, resulting into fake phase jumps. For this, we apply very small random perturbations to filter design parameters, which move the zeros and poles of its transfer function.

The zero-pole plot of the utilized prototype IIR filter (see Section 3.1) and the region span by its perturbed zeros and poles are illustrated in Fig. 5(c). It is known that all Elliptic IIR filter

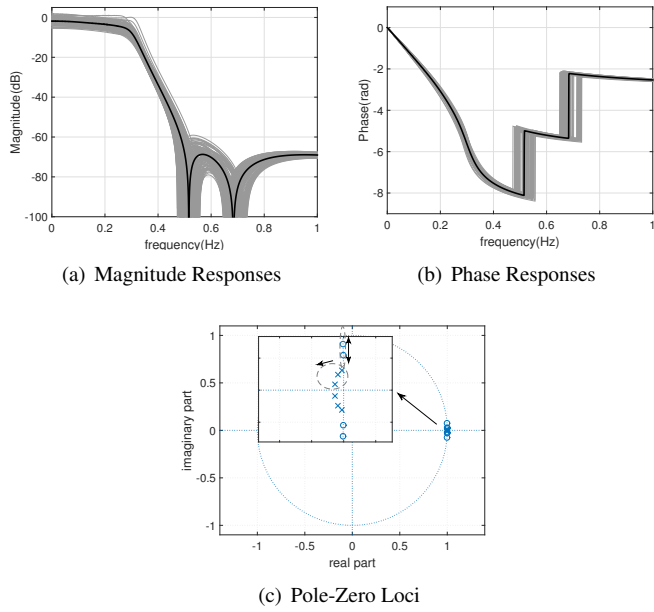


Figure 5: (a) and (b) The frequency responses (magnitude and phase respectively) of 100 lowpass prototype filters obtained by pole-zero perturbation. (c) Zero-pole plot of the prototype Elliptic IIR filter. The contours specify the areas of random movements of zeros and poles.

zeros are located on the unit-circle. Thus, to prevent any major changes in the filter’s characteristics, these zeros are perturbed randomly only on the unit-circle. For this, the filter’s zeros are taken into polar coordinates  $(\rho, \theta)$ , and the random perturbations are applied only to  $\theta$ . Another important consideration is that any perturbation in the pole locations should not take the poles out of the unit-circle (to keep it stable). Hence, the poles were randomly perturbed inside the unit circle, as specified in Fig. 5(c). Finally, the conjugate symmetry of the zeros and poles should be preserved to guarantee the realness of the impulse response. The magnitude and phase response of 100 lowpass prototype filters obtained by the proposed pole-zero perturbation procedure are shown in Fig. 5(a) and Fig. 5(b), where we can see that the filter pole-zero perturbations have had rather minor impact on the filters’ response (irrelevant to most cerebral studies). However, it is later shown that even these minor changes can significantly change the EEG phase, especially during LAAS.

After applying the first three steps of the proposed method on a raw EEG segment, we obtain a number of frequency-specific instantaneous phase sequence ensembles. The next remaining steps are applied to obtain a robust estimate of the phase estimates.

### 3.4. Step (4): Phase Unwrapping

Calculating the phase by the four quadrant arc-tangent causes *phase-wrapping* [21]. The amplitude of this phase sequence can take any value and typically exceeds the range  $[-\pi, \pi]$ , which is returned by the arc-tangent function. In cases where the phase exceeds this range, it is wrapped so that it stays within the

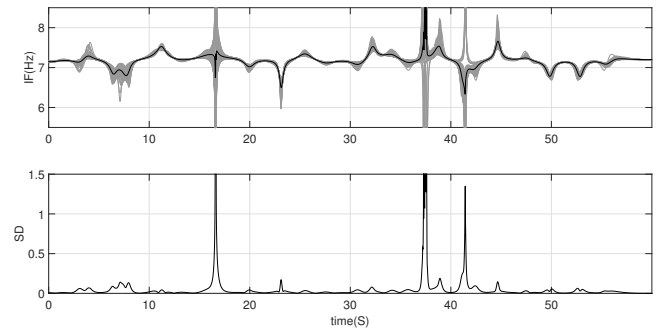


Figure 6: (top panel) The gray shades show ensembles of the estimated instantaneous frequency using 100 filters with minor pole-zero perturbations, and the final averaged instantaneous frequency in solid black line; (bottom panel) the standard deviation of the instantaneous frequency for 100 ensembles at each time instant.

normal range [21, 22]. In such cases, the wrapped phase sequence will contain some phase-jumps equal to  $\pm\pi$ . Therefore, for EEG phase analysis (either from the phase itself or from its time difference), an *unwrapping* procedure is required to obtain the phase sequence in its original form. An unwrapped phase sequence linearly diverges in time. For better illustration of the phase fluctuations, one may either subtract the constant linear phase signal  $\omega_0 t$  from the instantaneous phase to obtain its temporal fluctuations, or alternatively the time difference of the phase signal may be shown, which is proportional to its instantaneous frequency.

### 3.5. Step (5): Ensemble Averaging

The final step of the algorithm is to average over the randomized ensembles of phase sequences obtained from the different filter responses, to obtain an average phase estimate.

For illustration, Fig. 6 shows 100 ensembles of the instantaneous frequency of a sample EEG segment obtained by the aforementioned randomization scheme (zero-pole perturbation) for a center frequency of 7 Hz, and the average of the randomized ensembles. This figure illustrates the importance of the proposed scheme and the significance of the zero-pole perturbation. Accordingly, without this procedure (by simply calculating the phase from a single filtered signal, as in conventional methods), the obtained phase sequence is unreliable (not robust), since each set of filter parameters (even with minor differences) would lead to significantly different results, especially during the low analytical signal envelope epochs in which the standard deviation of the instantaneous frequency is significantly high (Fig. 6).

### 3.6. Example

In this section the robustness and reliability of the proposed method is verified versus conventional methods for a sample signal. The phase sequence of an EEG signal has been extracted using the proposed method and the conventional method (without parameter perturbation). The sample signal, represented in Fig. 7, is about 24 s of an ongoing EEG with the sampling frequency of  $f_s=173.61$  Hz, recorded during a BCI study. The

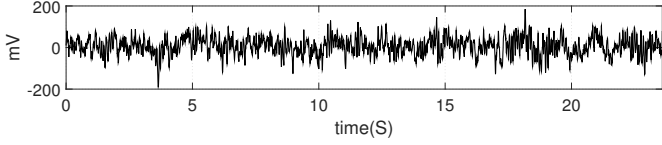


Figure 7: Utilized ongoing EEG signal to assess the robustness of the proposed phase estimation method.

complete description of the data is presented in [23]. In the following subsections, the phase robustness of this sample data is studied from three aspects: (1) effect of filter parameter variations, (2) robustness to noise and (3) low-amplitude analytic signal and phase jumps.

### 3.6.1. Filter Parameter Variations

For assessing the sensitivity of the proposed method to changes in filter parameters, the following three scenarios are tested using a lowpass Elliptic IIR filter design scheme:

1.  $f_0 = 7$  Hz,  $BW=0.5$  Hz (pass-band bandwidth),  $TB=0.5$  Hz (transition-band from either side),  $f_s=173.61$  Hz, 0.1 dB maximum pass-band ripple and 70 dB minimum stop-band attenuation
2.  $f_0 = 7$  Hz,  $BW=0.2$  Hz,  $TB=0.2$  Hz  $f_s=173.61$  Hz, 0.1 dB maximum pass-band ripple and 70 dB minimum stop-band attenuation
3.  $f_0 = 7$  Hz,  $BW=1.0$  Hz,  $TB=1.0$  Hz  $f_s=173.61$  Hz, 0.1 dB maximum pass-band ripple and 70 dB minimum stop-band attenuation

where  $TB$  represents the transition band. The instantaneous frequency obtained from (7) for these three cases are shown in Fig. 8 using both the conventional and proposed methods. It can be seen that the conventional method is very sensitive to variations in filter's parameters and with minor changes in the bandpass filter design parameters, the results have significantly changed. Nevertheless, the presented method shows more stable results to changes in filter's parameters, since the filter parameter effects are almost removed through perturbing the filter's frequency response and averaging between the perturbed ensembles.

### 3.6.2. Noise Susceptibility

To investigate the robustness of the proposed method to noise, once again the instantaneous frequency is estimated from the previous EEG signal using a bandpass filter  $f_0 = 7$  Hz,  $BW=0.5$  Hz, and  $TB=0.5$  Hz, in three levels of *additive white Gaussian noise* (AWGN):

1. No noise (pure EEG)
2. Contaminated by AWGN with SNR= 10 dB
3. Contaminated by AWGN with SNR= 0 dB

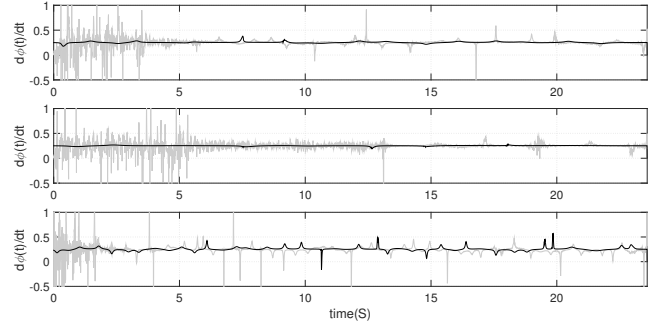


Figure 8: Instantaneous frequency around  $f_0=7$  Hz calculated by the conventional (gray) and proposed method (black) for three filter parameter sets described in Section 3.6.1 (from top to bottom)

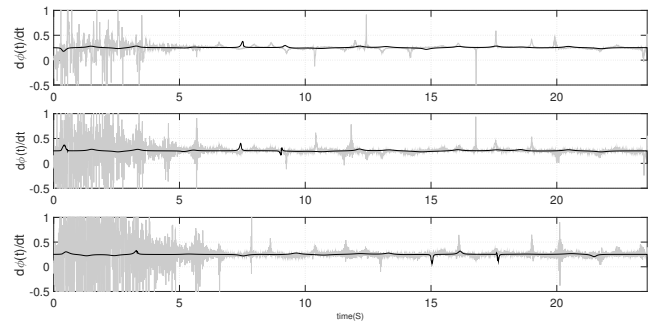


Figure 9: Instantaneous frequency calculated through the conventional (light gray) and proposed method (black) for 1) noiseless, 2) AWGN with SNR= 10 dB, and 3) AWGN with SNR= 0 dB (from top to bottom).

The corresponding results are shown in Fig. 9 for both the conventional and presented methods. It can be seen that the conventional method, regardless of the large spikes at the beginning (due to transient effects), has significant variations and spikes under AWGN. Clearly, the conventional phase estimation procedure is unreliable during noisy epochs. Nevertheless, the proposed method has been rather robust to background noise. A rigorous discussion on the effect of noise and SNR level on the probability of correct and false phase detections was presented in [11].

### 3.6.3. Low-amplitude Analytic Signal and Phase Jumps

Fig. 10 shows the instantaneous frequency and the instantaneous analytical signal envelope calculated for the sample EEG in Fig. 7 using conventional methods, for frequency components in the range of DC to 30 Hz, using the three filtering schemes stated in Section 3.6.1. The same procedure is performed using the proposed method and the results are depicted in 11 for comparison. The comparison of Fig. 10 and Fig. 11, clearly shows the effects of LAAS on the EEG phase jumps using the classical and proposed methods. It is seen that the phase sequences estimated by conventional methods are prone to fake jumps at points where the corresponding analytic signal have lower amplitudes; while this issue has been significantly improved using the proposed method.

Figure 12 shows the instantaneous frequency and the instan-

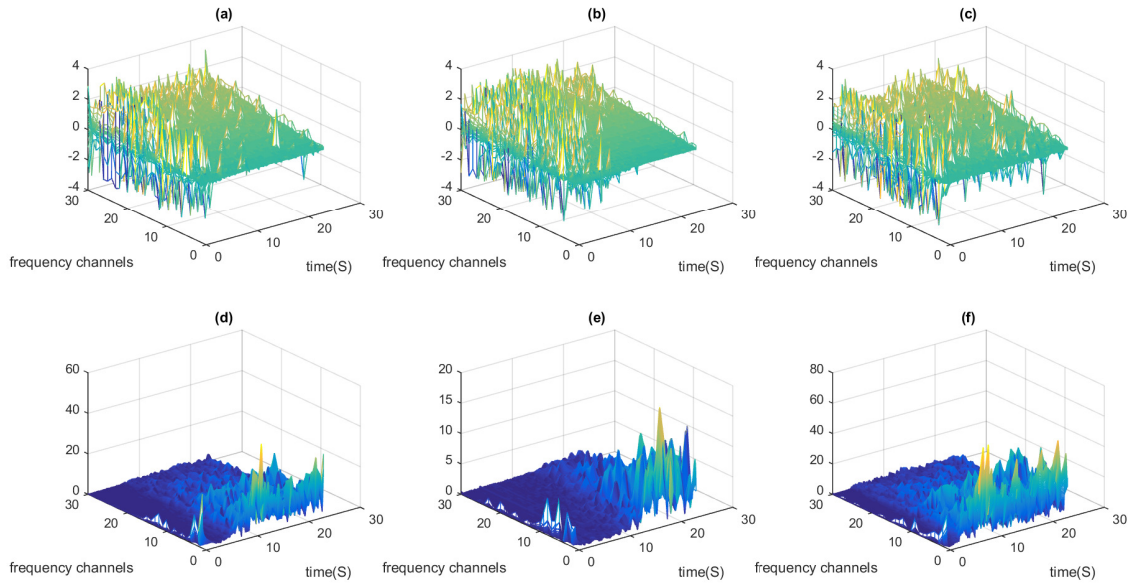


Figure 10: The instantaneous frequency (top row) and the corresponding instantaneous amplitudes (bottom row), calculated from the EEG signal shown in Fig. 7 through the *conventional phase extraction procedure*, for frequency components in the range of DC to 30 Hz and using three different sets of filter parameters 1)  $BW=0.5$  Hz,  $TB=0.5$  Hz, 2)  $BW=0.2$  Hz,  $TB=0.2$  Hz and 3)  $BW=1.0$  Hz,  $TB=1.0$  Hz from left to right, respectively.

taneous analytical signal envelope calculated for the sample EEG in Fig. 7 using conventional methods, for frequency components in the range of DC to 30 Hz, using three different noise levels stated in Section 3.6.2. The same procedure is repeated using the proposed method and the results are depicted in 13 for comparison, where we can see that the proposed method has been considerably less susceptible to additive noise.

#### 4. Case Study: Phase and Frequency Features for a Brain Computer Interface Application

##### 4.1. Problem Definition

In order to show the significance of the proposed method, its performance is evaluated in a *visual evoked potential (VEP)*-based BCI system, as proof of concept. The state-of-the-art classification procedure used in previous VEP-based BCI studies is employed for this purpose [16, 24, 25], and we focus on the impact of EEG phase feature using conventional versus the proposed scheme. The details of the studied case study are described below. It should be noted that this case study is only presented as a typical application for extracting reliable EEG phase sequences and not for improving the classification rates in state-of-the-art BCI systems.

##### 4.1.1. Dataset

The dataset used for this study is adopted from the *Neuroelectric and Myoelectric Databases*, which is online available on Physionet [26]. This dataset includes one- and two-minute recordings of 109 volunteers performing a series of motor and motor-imagery tasks. Each record contains sixty four channels of EEG recorded using the *BCI2000 System*, during a set of

annotated mental tasks [27]. The complete description of the dataset is available at [26]. Each subject performed a series of mental tasks: two one-minute baseline runs, with open and closed eyes and three two-minute runs of four different tasks as described below:

1. A target appears on the *left or right* side of a screen in front of the subject. The subject opens and closes the corresponding fist until the target disappears. Then the subject relaxes.
2. A target appears on the *left or right* side of the screen. The subject *imagines* opening and closing the corresponding fist until the target disappears. Then the subject relaxes.
3. A target appears on the *top or bottom* of the screen. The subject opens and closes both fists (if the target is on top) or both feet (if the target is on the bottom) until the target disappears. Then the subject relaxes.
4. A target appears on the *top or bottom* of the screen. The subject *imagines* opening and closing both fists (if the target is on top) or both feet (if the target is on the bottom) until the target disappears. Then the subject relaxes.

Fig. 14 shows the placement of the electrodes used to record EEG signals in this dataset. Since the primary cortical regions involved in the task of motor imagery are the *supplementary motor area (SMA)* and the *primary motor cortex (M1)* area, electrodes FCz, C3, and C4 are chosen for this study [16, 28, 29].

The annotations provided by the providers of the dataset consist of three classes, for identifying rest, versus left/up or

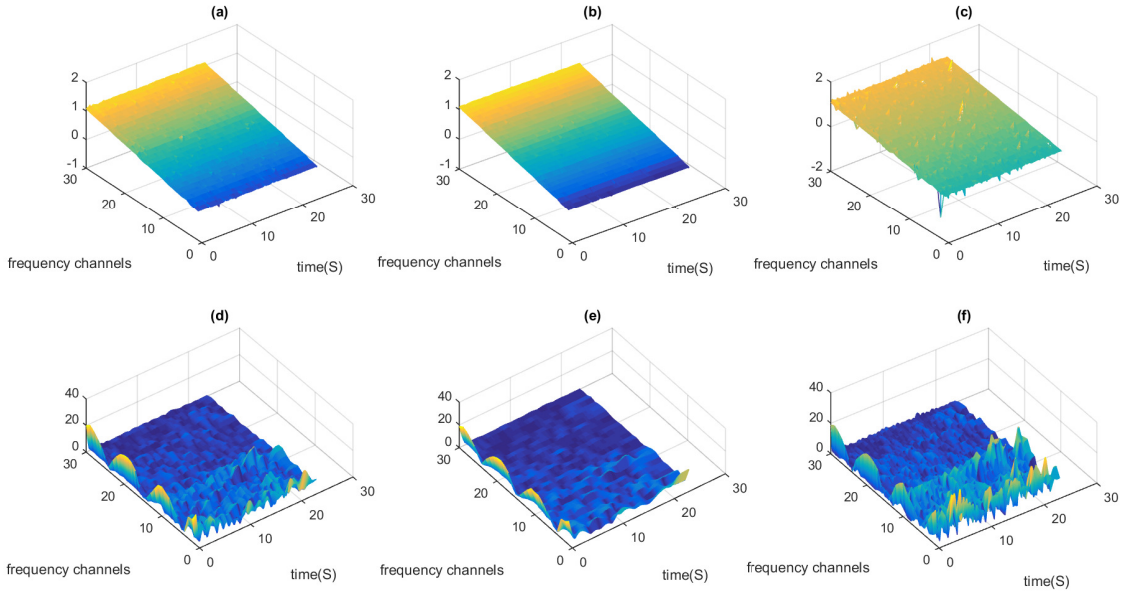


Figure 11: The instantaneous frequency (top row) and the corresponding instantaneous amplitudes (bottom row), calculated from the EEG signal shown in Fig. 7 through the *proposed phase extraction procedure*, for frequency components in the range of DC to 30 Hz and using three different sets of filter parameters 1)  $BW=0.5$  Hz,  $TB=0.5$  Hz, 2)  $BW=0.2$  Hz,  $TB=0.2$  Hz and 3)  $BW=1.0$  Hz,  $TB=1.0$  Hz from left to right, respectively.

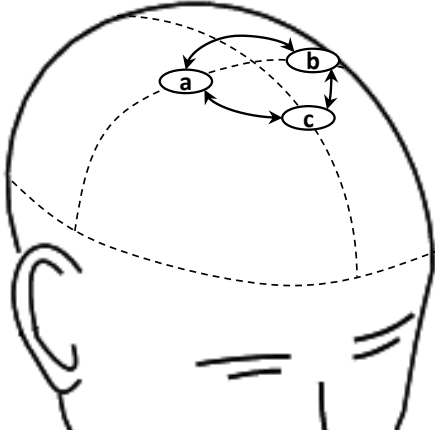


Figure 14: The location of the three (out of sixty four) leads used for the BCI classification case study. (a), (b) and (c) represent C4, C3 and FCz, respectively.

right/down side activities: 1)  $T_0$  corresponding to *rest* condition, 2)  $T_1$  corresponding to motion (real or imagined) onset of either the *left fist* or *both fists*, and 3)  $T_2$  corresponding to motion (real or imagined) onset of either the *right fist* or *both feet*. We therefore have a three-class classification problem. The targets appeared on the screen every four seconds, resulting in thirty 4 s annotated EEG segments in each of the two minute recordings (per subject), each corresponding to a mental task trial.

#### 4.1.2. Feature Extraction

A survey of previous studies on VEP-based BCI systems reveals that EEG phase-related features, are currently among the

most discriminative and informative features for BCI applications [16, 24, 30]. During feature extraction, a broad range of features are commonly extracted from the frequency band of interest and passed to the feature selection and classification stages. However, in this study only one phase-related feature, namely the PLV, is used to evaluate the robustness and feasibility of the proposed instantaneous phase estimation procedure.

PLV is a measure for quantifying how constant the phase difference between two signals is. In order to calculate the PLV for two signals (or channels)  $x(t)$  and  $y(t)$ , the following steps are required [8, 10]:

- Using narrow-band filters centered at  $f$ , calculate the instantaneous frequency-specific phase values  $\phi_x(t, f)$  and  $\phi_y(t, f)$ .
- Calculate the instantaneous phase-difference between  $x(t)$  and  $y(t)$  and quantify the local stability of this phase-difference over time:

$$PLV(f) = \left| \frac{1}{T} \sum_{t=1}^T \exp(j[\phi_y(t, f) - \phi_x(t, f)]) \right| \quad (8)$$

where  $T$  is the signal length and the summation is over all temporal samples of the instantaneous phases.

PLV varies between 0 and 1, corresponding to completely non-synchronized signals and complete synchronization, respectively [8, 10].

In this case study, the EEG phase and the corresponding PLV features were extracted using both procedures (classical and proposed) from three different subjects of the introduced dataset. The PLV were calculated for a single frequency

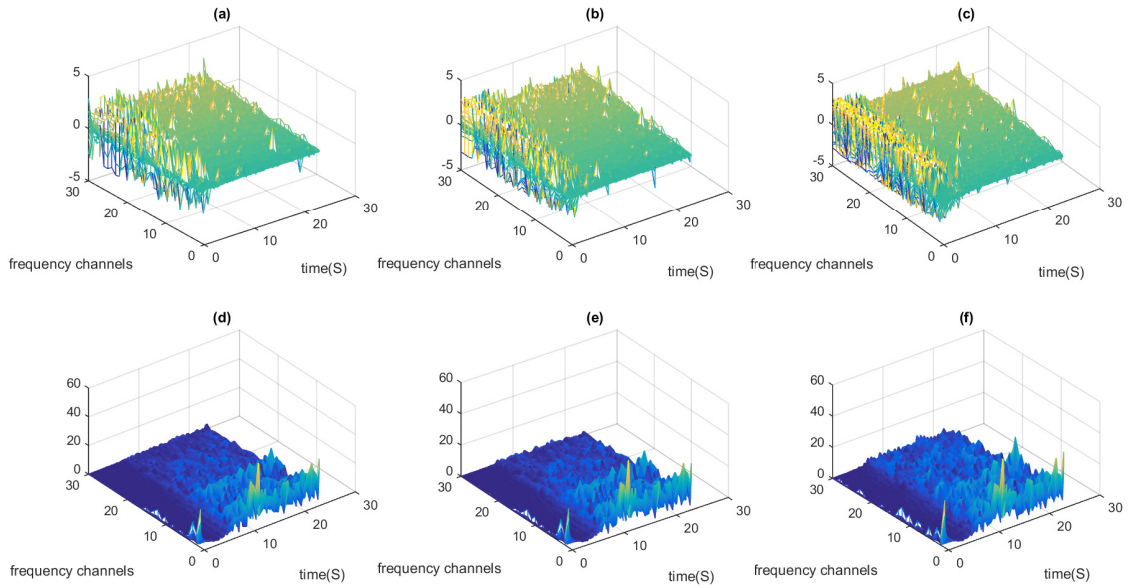


Figure 12: The instantaneous frequency (top row) and the corresponding instantaneous amplitudes (bottom row), calculated through the *conventional phase extraction procedure* for frequency components in the range of DC to 30 Hz for the sample EEG shown in Fig. 7, in three different cases: 1) no noise, 2) AWGN with SNR=10 dB, and 3) AWGN with SNR=0 dB from left to right, respectively.

band  $f = 7$  Hz, between all three possible combinations of selected electrodes, i.e., FCz-C3, FCz-C4 and C3-C4 (as shown in Fig. 14), resulting in feature vectors of length three. The feature vectors were computed from each of the thirty 4 s annotated temporal windows over all two-minutes records.

#### 4.1.3. Classification

The PLV feature vectors (calculated by both the conventional and proposed methods) together with the described annotations provided in the database were used for training and testing the classifiers. The *K-Nearest Neighbors* (KNN) with  $K=10$  (the number of nearest neighbors used in the classification), and *Random Forest* (RF) with number of trees equal to 10, were used as classifiers in a *leave-one-out* cross-validation process, in which, the feature-set of one subject is considered as test data and the rest of the feature sets are used for training the classifiers.

#### 4.2. Results

The comparison has been made both with and without considering additive noise (an additive white Gaussian noise with SNR=5 dB) to investigate the robustness of extracted features through both conventional and proposed procedures. The results of the noiseless and noisy cases are reported in Tables 1 and 2, respectively, for three typical subjects. Accordingly, the proposed method for extracting PLV features has significantly improved the classification rates as compared with conventional methods for extracting the EEG phase, both in absence and presence of additive noise.

In order to make the results reproducible, all source codes related to this study are online available in the open-source elec-

trophysiological toolbox (OSET) [31]<sup>2</sup>.

## 5. Discussion

The EEG Phase is a rich source of information for various fields of brain studies. Conventional methods for calculating the instantaneous phase and frequency of EEG signals are unreliable in presence of spontaneous background EEG activity and in low analytical signal envelopes [11]. Therefore, robust methods for phase calculation are required.

Herein a robust phase estimation procedure was proposed to overcome these issues. The proposed method has additional steps as compared to conventional methods: 1) zero-pole perturbation of the bandpass filters, 2) zero-phase filtering, and 3) ensemble averaging between the perturbed phase estimates for better robustness. The zero-pole perturbation decreases the effects of LAAS and provide a more reliable instantaneous phase sequence. However, as recently reported in [11], the phase ambiguities due to LAAS are unavoidable and should be considered as an intrinsic limitation for phase estimation. It was shown that the combination of the proposed methods, significantly reduces the sensitivity to noise and variations in filter parameters, which have been commonly neglected in previous studies.

For BCI applications, the results presented in Section 4 emphasize the significance and robustness of the proposed phase extraction procedure. The results show that phase-related features obtained through the proposed method not only outper-

<sup>2</sup>All source codes related to this paper shall be provided online after the publication of the current study.

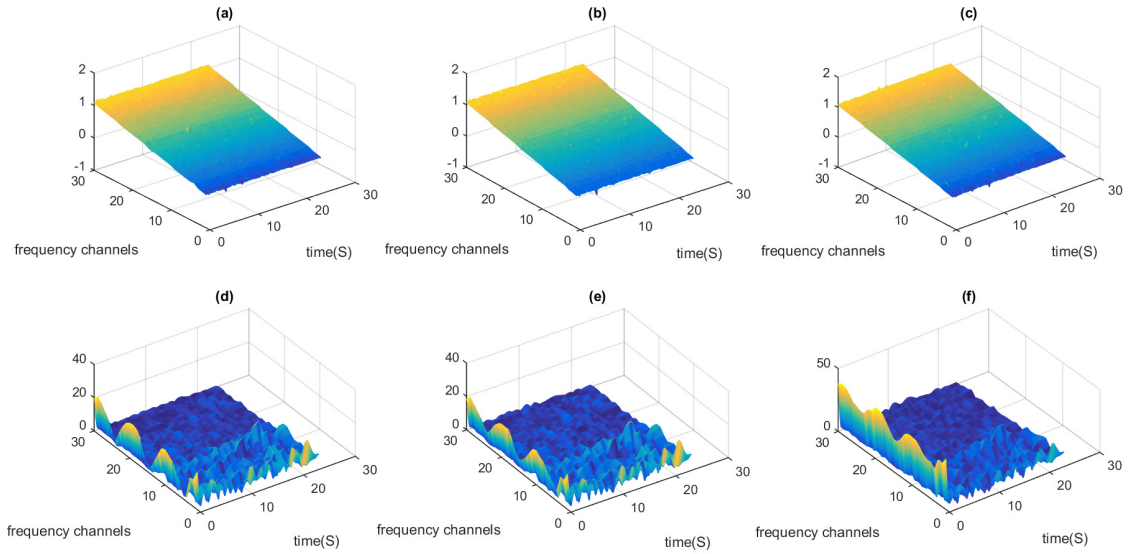


Figure 13: The instantaneous frequency (top row) and the corresponding instantaneous amplitudes (bottom row), calculated through the *proposed phase extraction procedure* for frequency components in the range of DC to 30 Hz for the sample EEG shown in Fig. 7, in three different cases: 1) no noise, 2) AWGN with SNR=10 dB, and 3) AWGN with SNR=0 dB from left to right, respectively.

Table 1: Classification Accuracy Per Subject and Mean Accuracy  $\pm$  Standard Deviation (%), Without Noise

	KNN		RF	
	Conventional	Proposed	Conventional	Proposed
S1	60.82	69.69	66.91	72.93
S2	61.90	69.82	68.83	73.38
S3	61.27	69.73	67.78	73.08
mean	$61.33 \pm 0.54$	$69.75 \pm 0.06$	$67.84 \pm 0.96$	$73.13 \pm 0.23$

form conventional phase features, but also are more robust to noise for BCI applications.

The scope of the proposed method is not limited to BCI applications. In fact, without using the hereby proposed scheme, the effects of LAAS and filtering schemes lead to unreliable and ambiguous phase sequences, which result in wrong interpretations of phase related quantities for applications which utilize EEG phase information (such as brain connectivity or BCI problems). This highlights the necessity of the mentioned additional steps to improve the reliability of the estimated instantaneous phase sequence of an EEG signal for different applications.

The theoretical findings of [11] and the hereby reported results highlight the importance of the analytical signal envelope in EEG phase-related studies. In future studies, the combination of phase and analytical signal envelopes can be used for improved performance in BCI and other applications.

## Acknowledgment

This research has been supported by the Cognitive Sciences and Technologies Council of Iran (COGC), under the grant number 2250.

## References

- [1] P. Y. Ktonas and N. Papp, "Instantaneous envelope and phase extraction from real signals: theory, implementation, and an application to eeg analysis," *Signal Processing*, vol. 2, no. 4, pp. 373–385, 1980.
- [2] F. Mormann, K. Lehnertz, P. David, and C. E. Elger, "Mean phase coherence as a measure for phase synchronization and its application to the eeg of epilepsy patients," *Physica D: Nonlinear Phenomena*, vol. 144, no. 3, pp. 358–369, 2000.
- [3] D. Rudrauf, A. Douiri, C. Kovach, J.-P. Lachaux, D. Cosmelli, M. Chavez, C. Adam, B. Renault, J. Martinerie, and M. Le Van Quyen, "Frequency flows and the time-frequency dynamics of multivariate phase synchronization in brain signals," *Neuroimage*, vol. 31, no. 1, pp. 209–227, 2006.
- [4] C. Brunner, B. Graimann, J. E. Huggins, S. P. Levine, and G. Pfurtscheller, "Phase relationships between different subdural electrode recordings in man," *Neuroscience Letters*, vol. 375, no. 2, pp. 69–74, 2005.
- [5] Y. Naruse, K. Takiyama, M. Okada, and H. Umehara, "Statistical method for detecting phase shifts in alpha rhythm from human electroencephalogram data," *Physical Review E*, vol. 87, no. 4, p. 042708, 2013.
- [6] P. Sauseng, W. Klimesch, W. Gruber, S. Hanslmayr, R. Freunberger, and M. Doppelmayr, "Are event-related potential components generated by phase resetting of brain oscillations? a critical discussion," *Neuroscience*, vol. 146, no. 4, pp. 1435–1444, 2007.
- [7] Z.-x. Zhou, B.-k. Wan, D. Ming, and H.-z. Qi, "A novel technique for phase synchrony measurement from the complex motor imaginary potential of combined body and limb action," *Journal of neural engineering*, vol. 7, no. 4, p. 046008, 2010.
- [8] J.-P. Lachaux, E. Rodriguez, J. Martinerie, F. J. Varela *et al.*, "Measuring

Table 2: Classification Accuracy Per Subject and Mean Accuracy  $\pm$  Standard Deviation (%), With Additive Noise

	KNN		RF	
	Conventional	Proposed	Conventional	Proposed
S1	58.00	68.55	65.09	72.03
S2	56.83	69.59	66.13	72.85
S3	58.32	69.41	65.94	72.30
mean	57.71 $\pm$ 0.79	69.19 $\pm$ 0.55	65.72 $\pm$ 0.56	72.40 $\pm$ 0.42

- phase synchrony in brain signals,” *Human brain mapping*, vol. 8, no. 4, pp. 194–208, 1999.
- [9] M. Le Van Quyen, J. Foucher, J.-P. Lachaux, E. Rodriguez, A. Lutz, J. Martinerie, and F. J. Varela, “Comparison of hilbert transform and wavelet methods for the analysis of neuronal synchrony,” *Journal of neuroscience methods*, vol. 111, no. 2, pp. 83–98, 2001.
- [10] M. G. Rosenblum, A. S. Pikovsky, and J. Kurths, “Phase synchronization of chaotic oscillators,” *Physical review letters*, vol. 76, no. 11, p. 1804, 1996.
- [11] R. Sameni and E. Seraj, “A Robust Statistical Framework for Instantaneous Electroencephalogram Phase and Frequency Analysis,” Aug. 2016, submitted to Elsevier NeuroImage (under review). [Online]. Available: <https://hal.archives-ouvertes.fr/hal-01355465>
- [12] B. Boashash, “Estimating and interpreting the instantaneous frequency of a signal. i. fundamentals,” *Proceedings of the IEEE*, vol. 80, no. 4, pp. 520–538, 1992.
- [13] B. Picinbono, “On instantaneous amplitude and phase of signals,” *IEEE Transactions on signal processing*, vol. 45, no. 3, pp. 552–560, 1997.
- [14] M. Chavez, M. Besserve, C. Adam, and J. Martinerie, “Towards a proper estimation of phase synchronization from time series,” *Journal of neuroscience methods*, vol. 154, no. 1, pp. 149–160, 2006.
- [15] J. Fell and N. Axmacher, “The role of phase synchronization in memory processes,” *Nature reviews neuroscience*, vol. 12, no. 2, pp. 105–118, 2011.
- [16] D. J. Krusienski, D. J. McFarland, and J. R. Wolpaw, “Value of amplitude, phase, and coherence features for a sensorimotor rhythm-based brain–computer interface,” *Brain research bulletin*, vol. 87, no. 1, pp. 130–134, 2012.
- [17] W. J. Freeman, “Origin, structure, and role of background eeg activity. part 2. analytic phase,” *Clinical Neurophysiology*, vol. 115, no. 9, pp. 2089–2107, 2004.
- [18] F. Mormann, T. Kreuz, R. G. Andrzejak, P. David, K. Lehnertz, and C. E. Elger, “Epileptic seizures are preceded by a decrease in synchronization,” *Epilepsy research*, vol. 53, no. 3, pp. 173–185, 2003.
- [19] M. D. Lutovac, D. V. Tošić, and B. L. Evans, *Filter design for signal processing using MATLAB and Mathematica*. Miroslav Lutovac, 2001.
- [20] A. V. Oppenheim and R. W. Schaffer, *Discrete-time signal processing*. Pearson Higher Education, 2010.
- [21] K. Itoh, “Analysis of the phase unwrapping algorithm,” *Appl. Opt.*, vol. 21, no. 14, p. 2470, 1982.
- [22] D. C. Ghiglia and M. D. Pritt, *Two-dimensional phase unwrapping: theory, algorithms, and software*. Wiley New York, 1998, vol. 4.
- [23] R. G. Andrzejak, K. Lehnertz, F. Mormann, C. Rieke, P. David, and C. E. Elger, “Indications of nonlinear deterministic and finite-dimensional structures in time series of brain electrical activity: Dependence on recording region and brain state,” *Physical Review E*, vol. 64, no. 6, p. 061907, 2001.
- [24] W. He, P. Wei, Y. Zhou, and L. Wang, “Combination of amplitude and phase features under a uniform framework with emd in eeg-based brain–computer interface,” in *2012 Annual International Conference of the IEEE Engineering in Medicine and Biology Society*. IEEE, 2012, pp. 1687–1690.
- [25] G. Townsend and Y. Feng, “Using phase information to reveal the nature of event-related desynchronization,” *Biomedical Signal Processing and Control*, vol. 3, no. 3, pp. 192–202, 2008.
- [26] A. L. Goldberger, L. A. Amaral, L. Glass, J. M. Hausdorff, P. C. Ivanov, R. G. Mark, J. E. Mietus, G. B. Moody, C.-K. Peng, and H. E. Stanley, “Physiobank, physiotoolkit, and physionet components of a new research resource for complex physiologic signals,” *Circulation*, vol. 101, no. 23, pp. e215–e220, 2000.
- [27] G. Schalk, D. J. McFarland, T. Hinterberger, N. Birbaumer, and J. R. Wolpaw, “Bci2000: a general-purpose brain–computer interface (bci) system,” *IEEE Transactions on biomedical engineering*, vol. 51, no. 6, pp. 1034–1043, 2004.
- [28] Q. Wei, Y. Wang, X. Gao, and S. Gao, “Amplitude and phase coupling measures for feature extraction in an eeg-based brain–computer interface,” *Journal of Neural Engineering*, vol. 4, no. 2, p. 120, 2007.
- [29] Y. Wang, B. Hong, X. Gao, and S. Gao, “Phase synchrony measurement in motor cortex for classifying single-trial eeg during motor imagery,” in *Engineering in Medicine and Biology Society, 2006. EMBS’06. 28th Annual International Conference of the IEEE*. IEEE, 2006, pp. 75–78.
- [30] J. Pan, X. Gao, F. Duan, Z. Yan, and S. Gao, “Enhancing the classification accuracy of steady-state visual evoked potential-based brain–computer interfaces using phase constrained canonical correlation analysis,” *Journal of neural engineering*, vol. 8, no. 3, p. 036027, 2011.
- [31] R. Sameni, “Oset: The open-source electrophysiological toolbox,” 2012.